Journal of Molecular Neuroscience (2021) 71:1761–1771
https://doi.org/10.1007/s12031-021-01872-0

miR-129-5p Ameliorates Ischemic Brain Injury by Binding to SIAH1 and Activating the mTOR Signaling Pathway

Yu Lei[1] · Xiaoyuan Jin[1] · Mingli Sun[1] · Zhiyong Ji[1]

Received: 4 May 2021 / Accepted: 9 June 2021 / Published online: 5 August 2021

Abstract

Aberrant expression of microRNAs (miRNAs) has been linked with ischemic brain injury (IBI), but the mechanistic actions behind the associated miRNAs remain to be determined. Of note, miR-129-5p was revealed to be downregulated in the serum of patients with IBI. In silico prediction identified a putative target gene, siah E3 ubiquitin protein ligase 1 (SIAH1), of miR-129-5p. Accordingly, this study plans to clarify the functional relevance of the interplay of miR-129-5p and SIAH1 in IBI. IBI was modeled by exposing human hippocampal neuronal cells to oxygen–glucose deprivation (OGD) in vitro and by occluding the middle cerebral artery (MCAO) in a mouse model in vivo. Apoptosis of hippocampal neuronal cells was assessed by annexin V-FITC/PI staining and TUNEL staining. The area of cerebral infarction was measured using TTC staining, along with neurological scoring on modeled mice. Loss of hippocampal neuronal cells in the peri-infarct area was monitored using Nissl staining. Downregulated miR-129-5p expression was found in OGD-induced hippocampal neuronal cells and MCAO-treated mice. Mechanistically, miR-129-5p was validated to target and inhibit SIAH1 through the application of dual-luciferase reporter assay. Additionally, enforced miR-129-5p inhibited the apoptosis of OGD-induced cells and decreased the cerebral infarct area, neurological scores and apoptosis of hippocampal neuronal cells by downregulating SIAH1 and activating the mTOR signaling pathway. Taken together, the results of this study reveal the important role and underlying mechanism of miR-129-5p in IBI, providing a promising biomarker for preventive and therapeutic strategies.

Keywords Ischemic brain injury · Neuronal cells · microRNA-129-5p · SIAH1 · mTOR signaling pathway

Introduction

Ischemic brain injury (IBI) can be caused by numerous events, including head trauma, cardiac arrest and stroke, which are associated with cortical dysfunctions (Li et al. 2020). IBI can lead to neuron-related functional impairment and further induce irreversible damage to neuronal cells and the brain, being involved in complicated pathological processes such as apoptosis, inflammation and oxidative stress (Wu et al. 2020). A great number of IBI patients suffer from insufficient cerebral blood supply, which eventually leads to cerebral infarction, and it has been reported that the 5-year recurrence risk of cerebral ischemia is 15–40% (Peng et al. 2019). Therefore, potential novel strategies to prevent and treat IBI are urgently needed.

✉ Zhiyong Ji
jizy@jlu.edu.cn

[1] Department of Critical Care Medicine, The First Hospital of Jilin University, Changchun 130000, P. R. China

MicroRNAs (miRNAs) modulate gene expression post-transcriptionally (Saugstad 2010). miRNAs have been implicated in IBI and have been considered as therapeutic targets (Chen et al. 2020). As a previous work reported, miR-129-5p is a kind of matured miR-129, exerting neuroprotective effects on neuronal cells (Zhou et al. 2018). miR-129-5p was previously demonstrated to exert an inhibitory effect on autophagy alongside apoptosis of hydrogen peroxide-induced H9c2 cells by activating PI3K/AKT/mTOR signaling in ischemic heart disease (Zhang et al. 2018). Elevated miR-129-5p could help to blunt blood–spinal cord barrier damage and neuroinflammation to further prevent ischemia–reperfusion (Li et al. 2017). However, the detailed regulatory mechanism of miR-129-5p in IBI is largely unknown. Interestingly, bioinformatics analysis in the present study identified putative binding sites of miR-129-5p in the 3′UTR region of siah E3 ubiquitin protein ligase 1 (SIAH1), suggesting that the impact of miR-129-5p may be achieved by modulating SIAH1. In addition, SIAH1 is implicated in the progression of IBI, acting as a downstream

protein (Shang et al. 2012). Furthermore, translocation of glyceraldehyde-3-phosphate dehydrogenase (GAPDH) to the nucleus is SIAH1-dependent on glutamate stimulation, which is related to ischemia-induced neuronal damage (Zhai et al. 2014). The mTOR-related pathway has been widely analyzed in IBI (Zhu et al. 2020). However, further elaboration about how the mTOR pathway interacts with miR-129-5p or SIAH1 remains to be established.

This study is designed to clarify the interaction between miR-129-5p and SIAH1 in IBI. Analysis of miR-129-5p may help to uncover the potential molecular mechanisms of IBI and offer novel therapeutic targets.

Methods

Ethics Statement

All participants signed informed consent forms before enrollment in the study. The Ethics Committee of The First Hospital of Jilin University approved the protocols of our study, which strictly adhered to the principles set forth by the Declaration of Helsinki. Approval of the animal experiments involved in this study has been obtained from the Animal Ethics Committee of The First Hospital of Jilin University.

Bioinformatics Analysis

The downstream genes of miRNA were predicted using the websites miRWalk (binding = 1, energy ≦ − 25, accessibility < 0.01, au > 0.45; http://mirwalk.umm.uni-heidelberg.de/), TargetScan (total context + + score < − 0.2; http://www.targetscan.org/vert_71/) and miRDB (target score > 70; http://www.mirdb.org/). A Venn diagram was drawn to obtain the gene intersection. GeneMANIA (http://genemania.org/) was used to predict relevant genes and to construct the protein–protein interaction (PPI) network, and the Cytoscape platform (http://www.cytoscape.org/) was used to visualize the images and calculate the gene core degree to screen out the key downstream genes. TargetScan was employed to predict the binding site between miRNA and the downstream gene, and the potential mechanism of the key gene was screened out by referring to the literature. Additionally, the Multi Experiment Matrix (MEM; available at https://biit.cs.ut.ee/mem/index.cgi) was used for co-expression analysis, and the R language program was used for KEGG enrichment analysis.

Study Subjects

Acute IBI patients ($n = 28$; 17 male and 11 female; aged 36–74 years, with an average age of 54.04 ± 7.99 years) in our hospital from May 2014 to October 2017 were included in the IBI group. For all patients this was their first ischemic attack, and it had occurred within the past 24 h. Patients were classified as non-cardiogenic IBI (atherothrombotic, lacunar, cryptogenic and unexplained) according to the TOAST (Trial of Org 10,172 in Acute Stroke Treatment) classification criteria and diagnosed by cranial computed tomography (CT) and magnetic resonance imaging (MRI). Patients with severe hepatic and renal insufficiency, autoimmune disorders, cerebral hemorrhage, craniocerebral injury, brain tumors, recent infection, hematological diseases or thyroid diseases were excluded from the study. Healthy participants ($n = 30$; 12 female and 18 male, aged 42–62 years, with an average age of 52.02 ± 5.45 years) subjected to physical examination were included in the normal group. Vein blood (3 mL) was collected from each participant after fasting in the morning the day after admission (while the blood of healthy participants was taken on the physical examination day). Vein blood was centrifuged for 20 min, followed by the collection of supernatants, which were stored in an Eppendorf tube at − 80 °C.

Culture of Hippocampal Neuronal Cells

Isolation and culture of the primary neuronal cells was performed based on methods reported previously (Li et al. 2019). The hippocampal neuronal cells were isolated from the embryos (E18.5) of the C57BL/6 mice under an anatomical microscope. Subsequently, the hippocampal neuronal cells were washed with D-Hanks' solution under sterile conditions and then seeded into the culture dish coated with 50 mg/mL poly-l-lysine at the density of 1×10^6 cells/cm^2. Cells were then subjected to culture in nerve basic medium containing 1% glutamine, 2% B27 and 1% penicillin/streptomycin at a temperature of 37 °C with 5% CO_2. Five days later, the purity of neuronal cells was measured using NeuN immunofluorescence assay, and 95% cells in the culture were positive for NeuN.

Hippocampal neuronal cells were infected with lentivirus vectors LV5-GFP (#25,999; Addgene, Watertown, MA, USA) for gene overexpression or pSIH1-H1-copGFP (LV601B-1) for gene silencing. Hippocampal neuronal cells were immersed in virus (1×10^8 TU/mL) and administered OGD. Briefly, neuronal cells were subjected to cultivation in glucose-free Earle's balanced salt solution (EBSS) at a temperature of 37 °C and then incubated in an anaerobic incubator under conditions of 95% N_2, 5% CO_2 and 37 °C for 6, 12, 24 and 48 h. Hippocampal neuronal cells were then collected for subsequent experiments. Except for untreated neuronal cells for blank group and OGD-induced neuronal cells without other treatments for the OGD group, the OGD-induced neuronal cells were subjected to transductions of miR-129-5p mimic/inhibitor, SIAH1 overexpression plasmid (OE-SIAH1), and small interfering RNA (siRNA) targeting

SIAH1 plasmids (si-SIAH1-1 and si-SIAH1-2), as well as the corresponding negative controls (NCs) including mimic/inhibitor NC, OE-NC and si-NC.

Establishment of Ischemic Brain Injury Mouse Model

A middle cerebral artery occlusion (MCAO) model was induced using C57/BL6 mice (aged 8–10 weeks; weighing 22–25 g) purchased from Better Biotechnology Co., Ltd. (Nanjing, China) with 12 mice in each group. First, anesthesia was performed with the mice being intraperitoneally injected with 3% sodium pentobarbital. Following the mouse brain atlas (Paxinos and Franklin 2001. The Mouse Brain in Stereotaxic Coordinates, Second Edition (Deluxe), Academic Press, New York, 2001, ISBN 0–12-547,637-X), 4 μL of lentivirus (with titer of 2×10^8 IFU/mL) was injected into the intracerebral ventricle of mice using a brain stereotaxic apparatus and a stepper-motorized microsyringe. The needle was retained for 5–10 min. At 1 h post-MCAO modeling, mice were injected with agomiR or antagomiR. Mice were anesthetized using sodium pentobarbital (5%), with the right common carotid artery and the external (ECA) and internal carotid artery (ICA) being exposed. The sutures were adopted for ligation of the common carotid artery. A 7–0 monofilament nylon suture (0.22–0.23 mm in diameter) coated with silicone and having a round tip was gently inserted into the ICA through the ECA stump and advanced 10 ± 0.5 mm when the round tip arrived at the entrance to the right middle cerebral artery, whereupon a slight resistance could be felt. It was successfully occluded using laser Doppler flowmetry (PeriFlux 5000) (Li et al. 2019). Except for the sham-operated mice for the sham group, and MCAO mice without other treatments for the MCAO group, the MCAO mice were subjected to treatments of miR-129-5p agomiR, SIAH1 overexpression vector (OE-SIAH1) and Rheb overexpression vector (OE-Rheb) alongside the corresponding NCs, including agomiR NC and OE-NC.

CCK-8 Assay

Cells were cultured in 96-well plates, with 100 μL per well. After culture, 100 μL CCK-8 mixture solution (90 μL original medium and 10 μL CCK-8 solution) was added to each well. The cells were further incubated, and the optical density (OD) at 450 nm was measured every 30 min to calculate cell viability.

Neurological Scoring

The neurological function of mice in each group was evaluated according to a previously described method (Rossi et al. 2019). Twenty-four hours after MCAO reperfusion, the neurological impairment tests were conducted, including motor tests (hindlimb flexion, forelimb flexion and head movement, scored on a scale of 0–6), balance tests (score range 0–6), and abnormal movement tests (score range 0–2). Total scores of 1–4, 5–9 and 10–14 indicated slight, moderate and severe injury, respectively. Three researchers independently examined the neurological function.

Triphenyl Tetrazolium Chloride (TTC) Staining

The mice were euthanized at 24 h post-MCAO modeling. Brain tissues were sliced into 2-mm coronal sections. Each slice was subjected to 2% TTC solution staining at a temperature of 37 °C for 30 min. The infarcted region was pale, while the non-infarcted region was brick red. Thereafter, hemisphere areas were analyzed using ImageJ software. The infarcted area and total area in each slice were measured. The infarcted volume of each layer was calculated as the product of the infarcted area of each layer and layer thickness, and the total infarct volume was the sum of the infarcted volume of each layer. The infarction rate was total volume divided by infarcted volume.

TUNEL Staining

Paraffin-embedded tissues were sectioned into 5 μm thickness. Five sections of the mouse brain hippocampal tissues were deparaffinized, followed by 1% proteinase K dilution (50 μL), and then incubated in an incubator at a temperature of 37 °C for 30 min. Addition of 0.3% H_2O_2 methanol solution was used to eliminate the activity of endogenous peroxidase (POD). After 1-h incubation with TUNEL reaction solution in the dark, sections were cultured with 50 μL Converter-POD for 30 min and then 2% diaminobenzidine (DAB) for a period of 15 min. This reaction was terminated by the addition of distilled water when brownish-yellow nuclei appeared. After counterstaining with hematoxylin, sections were subjected to dehydration with gradient ethanol and mounted using balsam, followed by analysis under a light microscope at 400-fold magnification. Each slice was observed with 10 visual fields randomly taken. The brown-yellow nuclei indicated apoptotic cells, while blue nuclei were indicative of normal cells. The apoptotic rate of hippocampal neuronal cells was measured by the ratio of brown-yellow cells to blue cells.

Nissl Staining

After successful MCAO modeling, mice were perfused with the use of 4% paraformaldehyde in PBS via the heart, followed by the extraction of the brains. After being fixed with 4% paraformaldehyde and dehydrated using 20 and 30% sucrose solution, the brain tissues were sliced into 20-μm sections, followed by 1-h staining with 0.04% cresyl violet

dissolved in acetate buffer. Next, the sections were observed under a light microscope. Cell counting was performed on the peri-infarct area of MCAO mice using five sections of each brain tissue.

Annexin V/Propidium Iodide (PI) Staining

Forty-eight hours after cell transfection, a flow cytometer was used to carry out annexin V-FITC/PI double staining at an excitation wavelength of 488 nm. The results were reproducible in three independent experiments.

Western Blot Analysis

Total protein content was isolated from cells or tissues using high-efficiency RIPA lysis buffer (R0010). Centrifugation was performed at a temperature of 4 °C and 15,000 rpm for a period of 15 min to collect the supernatant, after which a BCA kit (20201ES76) was employed to measure the protein concentration in each sample. After separation, the proteins were transferred onto a polyvinylidene fluoride (PVDF) membrane, and the membrane was blocked by 5% bovine serum albumin (BSA) for a period of 1 h. Diluted primary rabbit anti-mouse antibodies to SIAH1 (ab155014, 1:1000), Rheb (ab25873, 1:1000), mTOR (ab2732, 1:1000), phosphorylated- (p-)mTOR (ab109268, 1: 5000), and p-S6K (9204, 1:1000) and S6K (ab9974, 1:1000) were obtained for incubation with the membrane overnight at a temperature of 4 °C. The membrane was further cultivated with goat anti-rabbit IgG (ab205718, 1:10,000) diluent labeled with horseradish peroxidase for a period of 1 h. All antibodies were obtained from Abcam (Cambridge, UK) except for p-S6K, which was purchased from Cell Signaling Technology (Danvers, MA, USA). The film was developed using Vilber FUSION FX5 (Vilber Lourmat, France), while proteins were quantified with ImageJ 1.48u software, followed by protein quantitative analysis.

RNA Extraction and Quantitation

TRIzol reagent (15,596,026, Invitrogen, Carlsbad, CA, USA) was employed for extraction of total RNA. Sample loading was performed with the use of the SYBR Premix Ex Taq kit (RR420A) by reverse transcription quantitative real-time polymerase chain reaction (RT-qPCR) in an Applied Biosystems ABI 7500 instrument. The employed primers were synthesized by Sangon Biotech (Table S1). The mRNA expression was measured via the $2^{-\Delta\Delta Ct}$ method with U6 and β-actin as endogenous references. U6 and hsa-miR-16 were taken as the internal references for miR-129-5p.

Luciferase Activity Assay

The WT and MUT of reporter plasmids (PmirGLO-SIAH1-WT, PmirGLO-SIAH1-MUT) containing binding sites with SIAH1 UTR were provided by GenePharma (Shanghai, China). The reporter plasmids were co-treated with mimic NC and miR-129-5p mimic into HEK293T cells, which were cultured for 48 h. The luminescent signal was monitored following the Dual-Luciferase detection kit (D0010) specifications. The Promega GloMax 20/20 Luminometer fluorescence detector (E5311) was applied to measure luciferase activity.

Flow Cytometry

Hippocampal neuronal cells were analyzed by detection on CD86 and CD206 antibodies via flow cytometry. Cells were cultured with anti-CD86/CD206 (1 μg/10^6 cells; AbD Serotec, Oxford, UK) supplemented with FITC at 4 °C for 30 min. After being fixed with 1% paraformaldehyde, cells were analyzed using the BD FACSCalibur flow cytometer. Nonspecific staining was removed using isotype-matched antibodies. At least 10,000 cells were collected for analysis using WinMDI 2.8 software.

Statistical Analysis

Statistical analysis for all data in the current study was carried out in SPSS 21.0 software. Measurement data were displayed as mean ± SD. Difference analysis between two groups of unpaired data with normal distribution and homogeneous variance was performed using the unpaired *t* test. Difference analysis among multiple groups was carried out using one-way analysis of variance (ANOVA) with Tukey's post-test. Analysis of the data at various time points was then performed via two-way ANOVA and Bonferroni tests. The Kruskal–Wallis test was employed for data processing of neurological deficit scores. A value of $p < 0.05$ was considered to indicate a statistically significant difference.

Results

Expression of miR-129-5p is Poor in Ischemic Brain Injury

We first detected miR-129-5p expression in clinical samples using RT-qPCR. It was found that miR-129-5p expression was lower in the serum of IBI patients than that of healthy participants ($p < 0.05$) (Fig. 1a). As shown in Fig. 1b, miR-129-5p expression gradually decreased in OGD-treated neuronal cells versus the control group. We also performed RT-qPCR to determine miR-129-5p expression in the brain

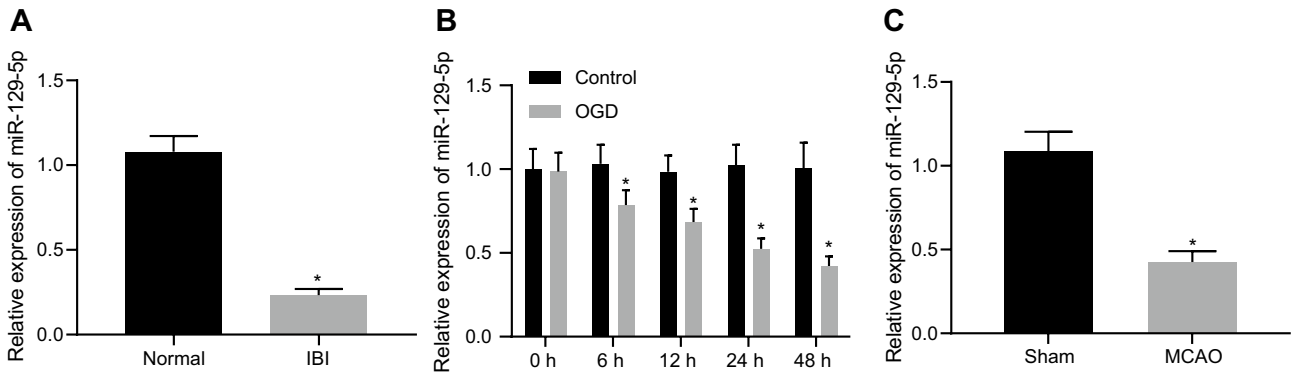

Fig. 1 Expression of miR-129-5p is reduced in IBI. **A** miR-129-5p level in serum of acute IBI patients ($n=28$) and healthy controls ($n=30$). * $p<0.05$ vs. healthy participants. **B** miR-129-5p expression in OGD-treated hippocampal neuronal cells and the control group detected by RT-qPCR. **C** Expression of miR-129-5p in brain tissues of MCAO mice and sham-operated mice detected by RT-qPCR. * $p<0.05$ vs. the control group. Data are shown as mean ± SD of three technical replicates. Two groups of data are compared using the unpaired *t* test; two-way ANOVA was employed for data analysis at varied time points

tissues of MCAO mice and sham-operated mice, the results of which suggested a decline in miR-129-5p expression in MCAO mice (Fig. 1c). These results provide evidence demonstrating that miR-129-5p expression is diminished in IBI.

Restored miR-129-5p Inhibits Apoptosis of OGD-induced Neuronal Cells in Vitro

To better understand the association between miR-129-5p and IBI, apoptosis of OGD-induced neuronal cells was analyzed. Annexin V-FITC/PI staining was performed 2 h after OGD treatment to detect cell apoptosis, while the CCK-8 assay was used to measure cell viability. The results showed that OGD treatment increased the rates of cell apoptosis and reduced cell viability. Moreover, OGD-induced cells following miR-129-5p mimic treatment significantly inhibited cell apoptosis and strengthened cell viability. However, OGD-induced cells following miR-129-5p inhibitor treatment demonstrated the opposite effects (Fig. 2a and b).

Western blot analysis carried out to detect protein levels of apoptosis-related factors revealed increased cleaved caspase-3 and Bax levels but decreased Bcl-2 levels in OGD-induced cells. Treatment with both OGD and miR-129-5p mimic led to reduced cleaved caspase-3 and Bax levels but increased Bcl-2 levels, while treatment with OGD and miR-129-5p inhibitor yielded the opposite effects (Fig. 2c). These results imply that miR-129-5p suppressed apoptosis of OGD-induced neuronal cells.

Restored miR-129-5p Inhibits Apoptosis of OGD-induced Neuronal Cells by Targeting SIAH1 in Vitro

To clarify the underlying mechanism of miR-129-5p in IBI, the databases miRWalk, TargetScan and miRDB were employed to determine the target genes of miR-129-5p. SIAH1 and ZNF704 were identified after the intersection of the plotted Venn diagram (Fig. 3a). The related genes of SIAH1 and ZNF704 were analyzed using GeneMANIA and a PPI network, showing that the core degree of SIAH1 in the PPI network was 47, which was calculated by Cytoscape. Also, the E3 ubiquitin protein ligase SIAH1 was involved in ubiquitination and proteasome-mediated degradation of specific proteins (Fig. 3b). Furthermore, the prediction results of the TargetScan database revealed that miR-129-5p bound SIAH1 in both humans and mice (Fig. 3c). In OGD-treated neuronal cells, SIAH1 expression was elevated (Fig. 3d). The targeting relationship between miR-129-5p and SIAH1 was verified by means of the dual-luciferase reporter (Fig. 3e). The level of SIAH1 was diminished in miR-129-5p mimic-treated cells, while an opposing trend was induced by miR-129-5p inhibitor (Fig. 3f). Thus, miR-129-5p negatively modulates the expression of SIAH1.

How miR-129-5p/SIAH1 affected apoptosis of hippocampal neuronal cells treated with OGD was subsequently illuminated. It was found that cell apoptosis was attenuated following co-treatment with OGD and miR-129-5p mimic, and the addition of OE-SIAH1 increased cell apoptosis. Cell apoptosis was reduced in OGD-induced cells treated with small interfering RNA targeting SIAH1 plasmids (si-SIAH1-1 and si-SIAH1-2) (Fig. 3g). Protein levels of SIAH1, cleaved caspase-3 and Bax were downregulated in OGD-treated cells treated with miR-129-5p, while Bcl-2 protein levels were upregulated. However, these results were reversed by OGD, miR-129-5p mimic and OE-SIAH1. In OGD-induced cells treated with si-SIAH1-1 and si-SIAH1-2, protein levels of SIAH1, cleaved caspase-3 and Bax decreased while that of Bcl-2 increased. The effects of si-SIAH1-1-treated cells were more obvious, which were selected for further analysis (Fig. 3h). It can be inferred that

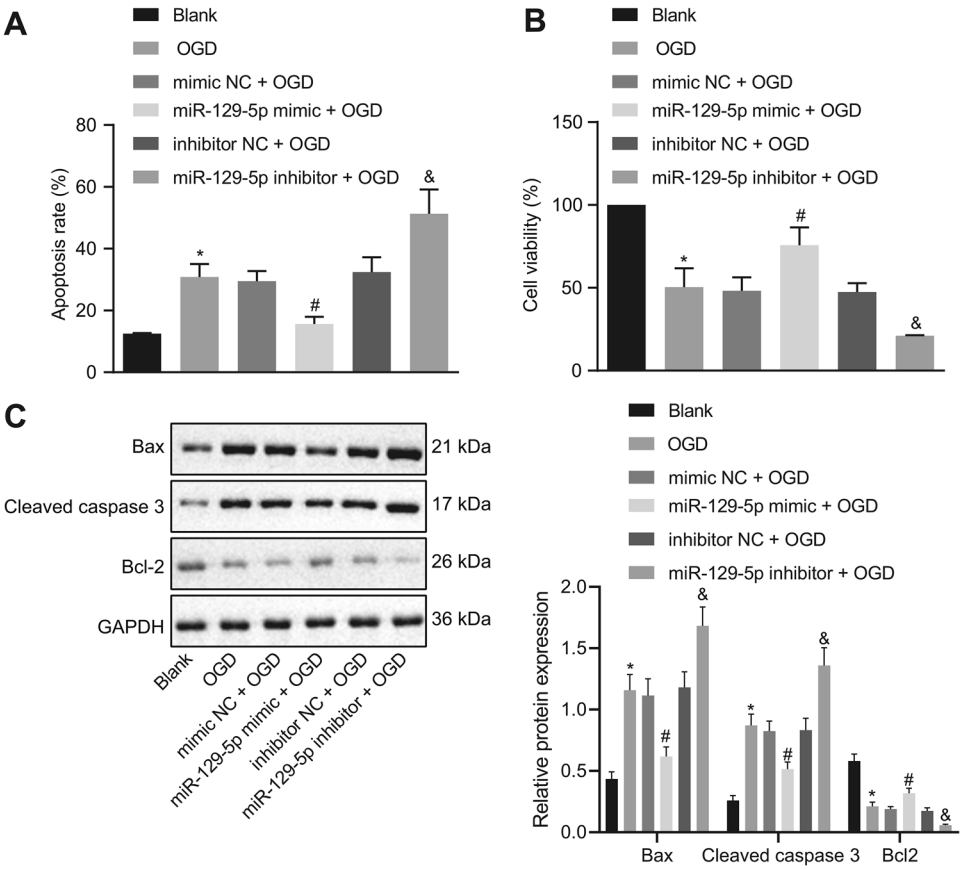

Fig. 2 Upregulation of miR-129-5p suppresses neuronal cell apoptosis triggered by OGD in vitro. **A, B** Cell apoptosis and cell viability in cells overexpressing or silencing miR-129-5p. **c** Protein levels of factors related to apoptosis in cells with altered expression of miR-129-5p. Data are shown as mean ± SD of three technical replicates, and analyzed by one-way ANOVA and Tukey's test. * $p < 0.05$ vs. the blank group. # $p < 0.05$ vs. OGD cells treated with mimic NC. &$p < 0.05$ vs. OGD cells treated with inhibitor NC

miR-129-5p protects OGD-induced hippocampal neuronal cells against IBI by downregulating SIAH1.

Restored miR-129-5p Ameliorates Ischemic Brain Injury by Downregulating SIAH1 in Vivo

IBI mouse models were established using MCAO to determine the effects of miR-129-5p/SIAH1 on IBI in vivo. Compared with sham-operated mice, the cerebral infarction area and neurological score of MCAO-treated mice were increased at 24 h after modeling, suggesting that the MCAO-treated mouse model was successfully constructed. TTC staining results revealed that the cerebral infarction area was diminished in miR-129-5p agomiR-treated MCAO mice, but was increased in the MCAO mice co-transfected with miR-129-5p agomiR and OE-SIAH1 (Fig. 4a). Furthermore, Nissl staining analysis revealed that miR-129-5p agomiR resulted in less hippocampal neuronal cell loss in the peri-infarct area in MCAO mice, which was opposite to the results caused by co-treatment with miR-129-5p agomiR and OE-SIAH1 (Fig. 4b). The results of neurological scoring revealed that miR-129-5p agomiR-treated MCAO mice displayed a lower score, while MCAO mice co-treated with miR-129-5p agomiR and OE-SIAH1 achieved a higher score (Fig. 4c). TUNEL assay showed that apoptosis of hippocampal neuronal cells was reduced in miR-129-5p agomiR-treated MCAO mice, but was increased in both miR-129-5p agomiR- and OE-SIAH1-treated MCAO mice (Fig. 4d). Subsequently, the expression of proteins related to apoptosis was examined using Western blot analysis after different treatments. The protein levels of SIAH1, Bax and cleaved caspase-3 were diminished in the miR-129-5p agomiR-treated MCAO mice, while the levels of Bcl-2 were increased. As for the MCAO mice co-treated with both miR-129-5p agomiR and OE-SIAH1, SIAH1, cleaved caspase-3 and Bax protein levels were elevated, while Bcl-2 levels were prominently reduced (Fig. 4e). These results suggest that miR-129-5p alleviates IBI by targeting SIAH1 in vivo.

SIAH1 Contributes to Ischemic Brain Injury by Inactivating the mTOR Pathway in Vitro and in Vivo

To conduct an in-depth study on the regulatory mechanism of miR-129-5p, we detected the downstream mechanism of SIAH1. A significant co-expression relationship between SIAH1 and Rheb was identified by MEM analysis (Fig. 5a). Moreover, 20 related genes of Rheb and the related PPI network were obtained by GeneMANIA prediction (Fig. 5b). It was confirmed that SIAH1 mainly affected IBI through

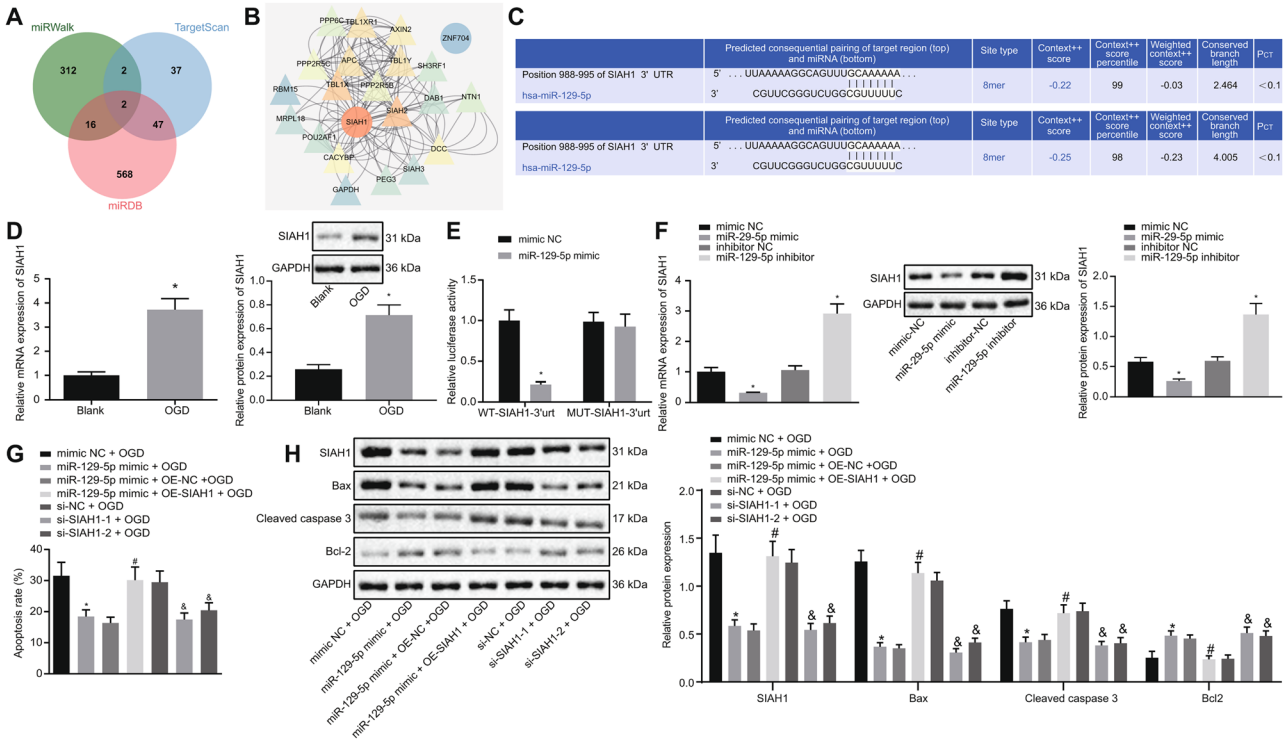

Fig. 3 miR-129-5p targets SIAH1 and prevents IBI in vitro. **A** Intersection of Venn diagram plotted using the prediction results of miRWalk, TargetScan and miRDB. **B** PPI network plotted by GeneMANIA. The circles represent SIAH1 and ZNF704, while triangles represent predicted related genes. Red represents a high core degree, while blue represents a low core degree. **C** Bindings sites between miR-129-5p and SIAH1 in humans (upper part) and mice (lower part). **D** mRNA (left histogram) and protein (right image and histogram) expression of SIAH1 in OGD-induced cells detected by RT-qPCR and Western blot analysis. * $p<0.05$ vs. the control group. **E** Targeting relationship verified by dual-luciferase reporter. * $p<0.05$ vs. mimic NC-treated cells. **F** mRNA (left histogram) and protein (right image) expression of miR-129-5p or SIAH1. * $p<0.05$ vs. mimic NC-treated cells. # $p<0.05$ vs. inhibitor NC-treated cells. **G** Cell apoptosis in cells treated with altered expression of miR-129-5p or SIAH1. **H** Protein levels of apoptosis-related factors in cells with altered expression of miR-129-5p or SIAH1. * $p<0.05$ vs. OGD-induced cells administered mimic NC. # $p<0.05$ vs. OGD-induced cells administered miR-129-5p mimic and OE-NC. & $p<0.05$ vs. OGD-induced cells administered si-NC. Data are shown as mean ± SD of three technical replicates. Two groups of data are compared by unpaired *t* test. Multiple groups of data are analyzed through one-way ANOVA and Tukey's test

the mTOR signaling pathway by KEGG enrichment and R language analyses of Rheb (Fig. 5c).

We examined the expression of SIAH1, Rheb and mTOR pathway-related genes in clinical samples of IBI using Western blot analysis. SIAH1 expression was found to be increased while the expression of Rheb, p-mTOR/mTOR and p-S6K/S6K was diminished in IBI (Fig. 5d). SIAH1 was found to be overexpressed or knocked down in the MCAO mouse models, whose efficiency was validated by RT-qPCR (Fig. 5e). In MCAO mice, SIAH1 protein expression was increased, while protein expression of Rheb, p-mTOR/mTOR and p-S6K/S6K was reduced. Furthermore, overexpressed SIAH1 by OE-SIAH1 also enhanced SIAH1 expression and diminished Rheb expression and p-mTOR/mTOR and p-S6K/S6K, while expression of Rheb, p-mTOR/mTOR and p-S6K/S6K increased slightly after simultaneous overexpression of SIAH1 and Rheb (Fig. 5f). The neurological scoring revealed that MCAO mice treated with OE-SIAH1 had higher scores, whereas MCAO mice co-treated with OE-SIAH1 and OE-Rheb displayed lower scores (Fig. 5g). The results of TTC and Nissl staining showed that in MCAO mice and the mice treated with both MCAO and OE-SIAH1, the cerebral infarction region and the loss of hippocampal neuronal cells in the peri-infarct area were increased. However, overexpression of both SIAH1 and Rheb induced the opposite effects on cerebral infarction area and loss of hippocampal neuronal cells in the peri-infarct area (Fig. 5h and i). In addition, as shown by the results of TUNEL staining, hippocampal neuronal apoptosis was significantly increased in MCAO mice and the mice treated with OE-SIAH1. In contrast, hippocampal neuronal apoptosis was decreased in MCAO mice co-treated with OE-SIAH1 and OE-Rheb (Fig. 5j). The above results indicate that SIAH1 reduces the transduction of mTOR signaling involved in the occurrence of IBI.

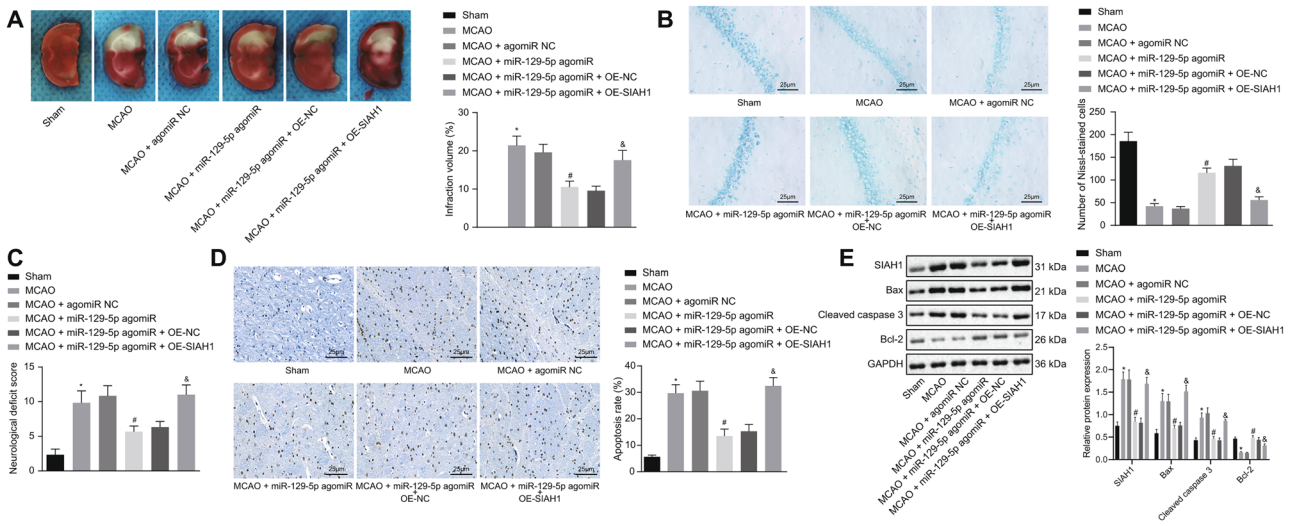

Fig. 4 Restored miR-129-5p relieves ischemic brain injury by downregulating SIAH1 in vivo. Sham-operated mice were used as controls and modeled mice were administered miR-129-5p agomiR or both miR-129-5p agomiR and OE-SIAH1. **A** Cerebral infarction area of mice ($n=12$) detected using TTC staining. **B** Loss of neuronal cells in mice ($n=12$) determined using Nissl staining (×400). **C** Neurological scoring of mice ($n=12$). **D** Cell apoptosis of mice ($n=12$) evaluated using TUNEL staining (×400). **E** Apoptosis-related proteins in mice ($n=12$). * $p<0.05$ vs. sham-operated mice. # $p<0.05$ vs. MCAO mice treated with agomiR NC. & $p<0.05$ vs. MCAO mice co-treated with miR-129-5p agomiR and OE-NC. Data are shown as mean ± SD and analyzed by one-way ANOVA and Tukey's test. Kruskal–Wallis test was employed for data processing in neurological deficit scores

Discussion

Accumulating evidence has highlighted the beneficial effects of miRNAs against brain damage, and specifically IBI (Zhao et al. 2013). Also, certain miRNAs can potentially serve as biomarkers to diagnose the diseases induced by cerebral ischemia/reperfusion (Chen et al. 2020). However, the functional role of miR-129-5p in IBI remains elusive. In the present study, we demonstrated that miR-129-5p-mediated protective effects are correlated with the suppression of SIAH1.

Firstly, miR-129-5p was found to be reduced in IBI. The biological properties can be mediated by miR-129 (Wu et al. 2019). Moreover, miR-129-5p downregulation has been identified in hippocampal neuronal cells of patients with Alzheimer's disease, and miR-129-5p can degrade the inflammatory reaction and suppress apoptosis of neuronal cells (Zeng et al. 2019). The results from our study also revealed that miR-129-5p inhibited apoptosis of neuronal cells induced by OGD. OGD is a common method for establishment of in vitro models of ischemia (Garrosa et al. 2020). Furthermore, neuronal apoptosis is responsible for IBI, which causes a number of serious health impairments (Ma et al. 2020). Upregulated miR-129-5p in the OGD-induced cell models resulted in downregulated Bax and cleaved caspase-3 protein levels but upregulated Bcl-2 levels. It is known that Bax and cleaved caspase-3 are proteins that promote apoptosis, and decreased Bax and cleaved caspase-3 levels indicate suppressed apoptosis (Ma et al. 2020). Therefore, miR-129-5p is expected to be a therapeutic target for IBI by controlling neuronal apoptosis.

We further investigated the downstream mechanism of miR-129-5p, discovering that SIAH1 was directly bound by miR-129-5p. The E3 ubiquitin protein ligase 1, SIAH1, is critical for GAPDH translocation from the cytoplasm to the nucleus (Tian et al. 2019). We found that SIAH1 was increased in OGD-induced neuronal cells (Fig. 3d), and loss of SIAH1 exerted inhibitory effects on neuronal apoptosis (Fig. 3g). The impacts of miR-129-5p and SIAH1 on MCAO-treated mice were also detected. Development of cerebral infarction is a sign of the development of cerebral ischemia (Zhang et al. 2020). In our current study, enforced miR-129-5p led to a decreased area of cerebral infarction, which was, however, reversed by upregulation of SIAH1. It was verified that miR-129-5p inhibited apoptosis of neuronal cells by mediating SIAH1. To our knowledge, we are the first to report the targeting association of miR-129-5p with SIAH1 in IBI.

Subsequently, our study showed that SIAH1 reduced the signal transduction of the mTOR pathway through Rheb degradation. As revealed a previous work, SIAH1 can lead to inactivated mTOR signaling by degrading Rheb, while stabilized Rheb, conversely, enhances mTOR signaling (Harraz et al. 2016). Rheb is a crucial mediator in myocardial ischemia, the knockdown of which can be used as a therapeutic marker for treatment (Sciarretta et al. 2012). Additionally, lower mTOR signaling can accelerate the

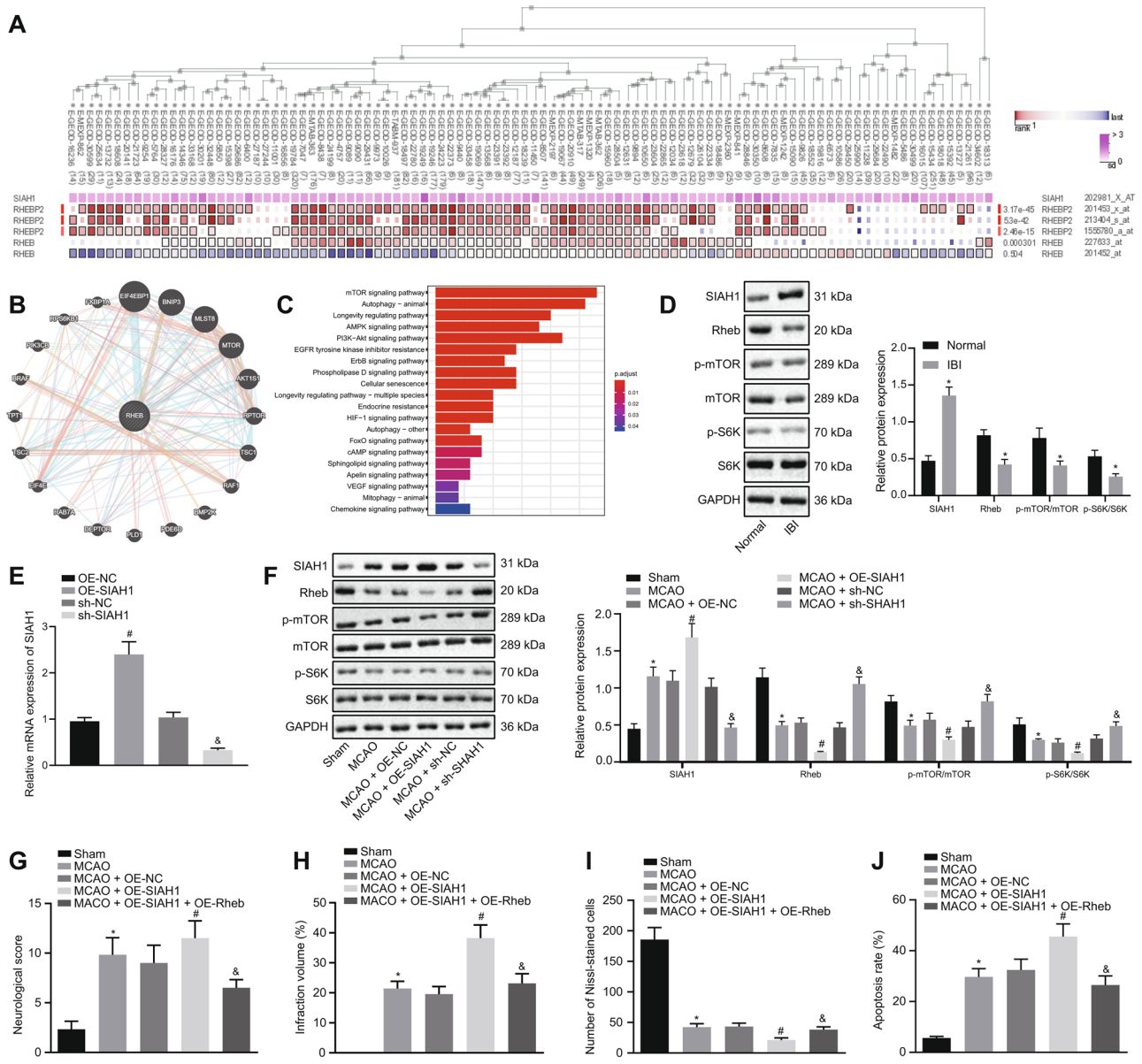

Fig. 5 SIAH1 contributes to ischemic brain injury by inactivating the mTOR pathway in vivo. **A** Co-expression of SIAH1 with Rheb predicted by MEM ($p = 3.013–04$). **B** PPI network of Rheb-related genes plotted by GeneMANIA. A larger circle represents a higher score in the PPI network. **C** KEGG enrichment of Rheb-related genes analyzed by R. The *Y*-axis represents the enriched pathway, while the *X*-axis indicates the number of genes enriched in the pathway. **D** Expression of Rheb, mTOR pathway-related genes (p-mTOR/mTOR and p-S6K/S6K). * $p < 0.05$ vs. the normal group. **E** Expression of SIAH1 in mice ($n = 12$). * $p < 0.05$ vs. the sham-operated mice. # $p < 0.05$ vs. MCAO mice treated with OE-NC. & $p < 0.05$ vs. the MCAO mice treated with si-NC. **F** Protein bands and levels of Rheb, p-mTOR/mTOR and p-S6K/S6K in mice ($n = 12$) assessed using Western blot analysis after different treatment. **G** Neurological scoring for mice ($n = 12$) after different treatment. **H** TTC staining results of cerebral infarction area in mice ($n = 12$). **i** Loss of neuronal cells in peri-infarct area of mice ($n = 12$) determined using Nissl staining. **J** Apoptosis of cells assessed using TUNEL staining. * $p < 0.05$ vs. sham-operated mice. # $p < 0.05$ vs. MCAO mice treated with OE-NC. & $p < 0.05$ vs. the MCAO mice treated with OE-SIAH1. Data are shown as mean ± SD. Two groups of data are compared by the unpaired *t* test. Multiple groups of data are compared by one-way ANOVA and Tukey's test. Kruskal–Wallis test was employed for data processing in neurological deficit scores

development of IBI (Xing et al. 2016). Consistently, our study also showed that degradation of Rheb by SIAH1 diminished mTOR signaling, thereby increasing the area of cerebral infarction in modeled mice.

In conclusion, the results of the current study suggest that miR-129-5p was reduced in OGD-treated neuronal cells and the MCAO-treated mouse model. Overexpression of miR-129-5p attenuated neuronal apoptosis in OGD-induced cells

and MCAO-treated mice. Additionally, it was shown that miR-129-5p accelerated the neuroprotective effects against IBI by targeting SIAH1. Therefore, the interplay between miR-129-5p and SIAH1 may be beneficial biomarkers for developing novel therapeutic and preventive strategies in IBI. However, whether the therapeutic target is applicable in humans requires further verification.

Supplementary Information The online version contains supplementary material available at https://doi.org/10.1007/s12031-021-01872-0.

Acknowledgements We acknowledge and appreciate our colleagues for their valuable suggestions and technical assistance for this study.

Authors' Contributions Yu Lei conceived and designed the study. Xiaoyuan Jin performed experiments and interpreted the results of experiments. Mingli Sun analyzed the data, prepared figures and drafted the paper. Zhiyong Ji edited and revised the manuscript. All authors read and approved the final manuscript.

Data Availability The datasets generated and/or analyzed during the current study are available from the corresponding author on reasonable request.

Declarations

Ethics statement All participants signed informed consent forms before enrollment in the study. The Ethics Committee of The First Hospital of Jilin University approved the protocols of our study, which strictly adhered to the principles set forth by the Declaration of Helsinki. Approval of the animal experiments involved in this study was obtained from the Animal Ethics Committee of The First Hospital of Jilin University.

Competing interests The authors declare that they have no competing interests.

References

Chen Z, Yang J, Zhong J, Luo Y, Du W, Hu C, Xia H, Li Y, Zhang J, Li M, Yang Y, Huang H, Peng Z, Tan X, Wang H (2020) MicroRNA-193b-3p alleviates focal cerebral ischemia and reperfusion-induced injury in rats by inhibiting 5-lipoxygenase expression. Exp Neurol 327:113223. https://doi.org/10.1016/j.expneurol.2020.113223

Garrosa J, Paredes I, Marambaud P, Lopez MG, Cano-Abad MG (2020) Molecular and Pharmacological Modulation of CALHM1 Promote Neuroprotection against Oxygen and Glucose Deprivation in a Model of Hippocampal Slices Cells 9. https://doi.org/10.3390/cells9030664

Harraz MM, Tyagi R, Cortes P, Snyder SH (2016) Antidepressant action of ketamine via mTOR is mediated by inhibition of nitrergic Rheb degradation. Mol Psychiatry 21:313–319. https://doi.org/10.1038/mp.2015.211

Li X, Zheng L, Xia Q, Liu L, Mao M, Zhou H, Zhao Y, Shi J (2019) A novel cell-penetrating peptide protects against neuron apoptosis after cerebral ischemia by inhibiting the nuclear translocation of annexin A1. Cell Death Differ 26:260–275. https://doi.org/10.1038/s41418-018-0116-5

Li XQ, Chen FS, Tan WF, Fang B, Zhang ZL, Ma H (2017) Elevated microRNA-129-5p level ameliorates neuroinflammation and blood-spinal cord barrier damage after ischemia-reperfusion by inhibiting HMGB1 and the TLR3-cytokine pathway. J Neuroinflammation 14:205. https://doi.org/10.1186/s12974-017-0977-4

Li Y, Ding R, Wang F, Guo C, Liu A, Wei L, Yuan S, Chen F, Hou S, Ma Z, Zhang Y, Cudmore RH, Wang X, Shen H (2020) Transient ischemia-reperfusion induces cortical hyperactivity and AMPAR trafficking in the somatosensory cortex. Aging (Albany NY) 12:4299–4321. https://doi.org/10.18632/aging.102881

Ma Q, Hou L, Gao X, Yan K (2020) NKAP promotes renal cell carcinoma growth via AKT/mTOR signalling pathway. Cell Biochem Funct 38:574–581. https://doi.org/10.1002/cbf.3508

Paxinos G, Franklin KBJ (2001) The mouse brain in stereotaxic coordinates, second ed. Academic Press, San Diego

Peng T, Jiang Y, Farhan M, Lazarovici P, Chen L, Zheng W (2019) Anti-inflammatory Effects of Traditional Chinese Medicines on Preclinical in vivo Models of Brain Ischemia-Reperfusion-Injury: Prospects for Neuroprotective Drug Discovery and Therapy. Front Pharmacol 10:204. https://doi.org/10.3389/fphar.2019.00204

Rossi V, Lispi M, Longobardi S, Mattei M, Di Rella F, Salustri A, De Felici M, Klinger FG (2019) Correction: LH prevents cisplatin-induced apoptosis in oocytes and preserves female fertility in mouse. Cell Death Differ 26:779. https://doi.org/10.1038/s41418-018-0174-8

Saugstad JA (2010) MicroRNAs as effectors of brain function with roles in ischemia and injury, neuroprotection, and neurodegeneration. J Cereb Blood Flow Metab 30:1564–1576. https://doi.org/10.1038/jcbfm.2010.101

Sciarretta S, Zhai P, Shao D, Maejima Y, Robbins J, Volpe M, Condorelli G, Sadoshima J (2012) Rheb is a critical regulator of autophagy during myocardial ischemia: pathophysiological implications in obesity and metabolic syndrome. Circulation 125:1134–1146. https://doi.org/10.1161/CIRCULATIONAHA.111.078212

Shang J, Liu N, Tanaka N, Abe K (2012) Expressions of hypoxic stress sensor proteins after transient cerebral ischemia in mice. J Neurosci Res 90:648–655. https://doi.org/10.1002/jnr.22776

Tian X, Gong L, Jin A, Wang Y, Zhou X, Tan Y (2019) E3 ubiquitin ligase siah1 nuclear accumulation is critical for homocysteineinduced impairment of C6 astroglioma cells. Mol Med Rep 20:2227–2235. https://doi.org/10.3892/mmr.2019.10449

Wu C, Zhang X, Chen P, Ruan X, Liu W, Li Y, Sun C, Hou L, Yin B, Qiang B, Shu P, Peng X (2019) MicroRNA-129 modulates neuronal migration by targeting Fmr1 in the developing mouse cortex. Cell Death Dis 10:287. https://doi.org/10.1038/s41419-019-1517-1

Wu L, Xiong X, Wu X, Ye Y, Jian Z, Zhi Z, Gu L (2020) Targeting Oxidative Stress and Inflammation to Prevent Ischemia-Reperfusion Injury. Front Mol Neurosci 13:28. https://doi.org/10.3389/fnmol.2020.00028

Xing G, Luo Z, Zhong C, Pan X, Xu X (2016) Influence of miR-155 on Cell Apoptosis in Rats with Ischemic Stroke: Role of the Ras Homolog Enriched in Brain (Rheb)/mTOR Pathway. Med Sci Monit 22:5141–5153. https://doi.org/10.12659/msm.898980

Zeng Z, Liu Y, Zheng W, Liu L, Yin H, Zhang S, Bai H, Hua L, Wang S, Wang Z, Li X, Xiao J, Yuan Q, Wang Y (2019) MicroRNA-129-5p alleviates nerve injury and inflammatory response of Alzheimer's disease via downregulating SOX6. Cell Cycle 18:3095–3110. https://doi.org/10.1080/15384101.2019.1669388

Zhai D, Chin K, Wang M, Liu F (2014) Disruption of the nuclear p53-GAPDH complex protects against ischemia-induced neuronal damage. Mol Brain 7:20. https://doi.org/10.1186/1756-6606-7-20

Zhang C, Zang Y, Hu L, Song Q, Zhao W, Zhang C, Liu H, Gu F (2020) Study on the risk prediction for cerebral infarction after transient ischemic attack: A STROBE compliant study.

Medicine (baltimore) 99:e19460. https://doi.org/10.1097/MD.0000000000019460

Zhang H, Zhang X, Zhang J (2018) MiR-129-5p inhibits autophagy and apoptosis of H9c2 cells induced by hydrogen peroxide via the PI3K/AKT/mTOR signaling pathway by targeting ATG14. Biochem Biophys Res Commun 506:272–277. https://doi.org/10.1016/j.bbrc.2018.10.085

Zhao H, Wang J, Gao L, Wang R, Liu X, Gao Z, Tao Z, Xu C, Song J, Ji X, Luo Y (2013) MiRNA-424 protects against permanent focal cerebral ischemia injury in mice involving suppressing microglia activation. Stroke 44:1706–1713. https://doi.org/10.1161/STROKEAHA.111.000504

Zhou XM, Liu J, Wang Y, Zhang SL, Zhao X, Xu X, Pei J, Zhang MH (2018) microRNA-129-5p involved in the neuroprotective effect of dexmedetomidine on hypoxic-ischemic brain injury by targeting COL3A1 through the Wnt/beta-catenin signaling pathway in neonatal rats. J Cell Biochem. https://doi.org/10.1002/jcb.26704

Zhu C, Zhou Q, Luo C, Chen Y (2020) Dexmedetomidine Protects Against Oxygen-Glucose Deprivation-Induced Injury Through Inducing Astrocytes Autophagy via TSC2/mTOR Pathway. Neuromolecular Med 22:210–217. https://doi.org/10.1007/s12017-019-08576-0